Acta Pharmacologica Sinica (2013) 34: 847–858
© 2013 CPS and SIMM All rights reserved 1671-4083/13 $32.00
www.nature.com/aps

Original Article

Allocryptopine and benzyltetrahydropalmatine block hERG potassium channels expressed in HEK293 cells

Kun LIN, Yu-qi LIU, Bin XU, Jin-liao GAO, Yi-cheng FU, Yu CHEN, Qiao XUE, Yang LI*

Institute of Geriatric Cardiology, the General Hospital of People's Liberation Army, Beijing 100853, China

Aim: Allocryptopine (ALL) is an alkaloid extracted from *Corydalis decumbens* (Thunb) Pers Papaveraceae, whereas benzyltetrahydropalmatine (BTHP) is a derivative of tetrahydropalmatine extracted from *Corydalis ambigua* (Pall) Cham et Schlecht. The aim of this study was to investigate the effects of ALL and BTHP on the human ether-a-go-go related gene (hERG) current expressed in HEK293 cells.
Methods: Cultured HEK293 cells were transiently transfected with hERG channel cDNA plasmid pcDNA3.1 using Lipofectamine. The whole-cell current IHERG was evoked and recorded using Axon MultiClamp 700B amplifier. The drugs were applied via supserfusion.
Results: Both ALL and BTHP reversibly suppressed the amplitude and density of I_{HERG} in concentration- and voltage-dependent manners (the respective IC_{50} value was 49.65 and 22.38 μmol/L). BTHP (30 μmol/L) caused a significant negative shift of the steady-state inactivation curve of I_{HERG}, while ALL (30 μmol/L) did not affect the steady-state inactivation of I_{HERG}. Furthermore, BTHP, but not ALL, shortened the time constants of fast inactivation and slow time constants of deactivation of I_{HERG}. But both the drugs markedly lengthened the time constants for recovery of I_{HERG} from inactivation. Using action potential waveform pulses, it was found that both the drugs at 30 μmol/L significantly suppressed the current densities in the late phase of action potential, but did not significantly affect the current densities in the early phase of action potential.
Conclusion: Both ALL and BTHP derived from Chinese herbs potently block hERG current.

Keywords: allocryptopine; benzyltetrahydropalmatine; hERG current; whole-cell patch-clamp recording; anti-arrhythmic agent

Acta Pharmacologica Sinica (2013) 34: 847–858; doi: 10.1038/aps.2012.176; published online 25 Mar 2013

Introduction

In ventricular myocytes, a pharmacological blockade of the 'rapid' delayed rectifier potassium current (I_{Kr}) and the current carried by its cloned equivalent, human ether-a-go-go related gene (hERG), can lead to ventricular action potential prolongation and QT interval prolongation in the electrocardiogram[1–3]. The pharmacological inhibition of hERG potassium channels is a property of class III antiarrhythmic drugs, such as amiodarone, sotalol and dofetilide[4, 5]. However, the excessive prolongation of the action potential duration (APD) leads to acquired long QT syndrome, which increases the risk of Torsades de Pointes (TdP) arrhythmias and sudden cardiac death. The assessment of direct hERG channel blockade has proven useful for evaluating drugs that are suspected of causing delays in cardiac repolarization and TdP[6–9]. The available anti-arrhythmic drugs and their narrow therapeutic indices have led researchers to explore the safety profile and effectiveness of alternative drugs.

Allocryptopine (ALL), a derivative of tetrahydropalmatine, is extracted from *Corydalis decumbens* (Thunb) Pers Papaveraceae (Figure 1A)[10–13]. Benzyltetrahydropalmatine (BTHP) is another derivative of tetrahydropalmatine that is extracted from the Chinese medicinal herb *Cryodalis amgibua* (Pall) Cham Et Schlecht (Figure 1B). Several previous studies have indicated that ALL and BTHP have potential antiarrhythmic effects in various animal models. Both of the drugs have electrophysiological effects that may contribute to the prolongation of the APD. In previous studies[14], we demonstrated that ALL possesses an inhibition effect on I_{to} in a frequency-dependent manner and decreases the transmural gradient of I_{to}. BTHP inhibits the I_{Kr} and the slowly delayed rectifier potassium current (I_{Ks}) in a frequency-dependent manner. It can be speculated that the use of ALL and BTHP as potential antiarrhythmic agents may be developed in the future[15–19]. However, little information is available on the effect of ALL and BTHP on hERG channels. We aimed to characterize the

* To whom correspondence should be addressed.
E-mail liyangbsh@163.com
Received 2012-08-20 Accepted 2012-11-28

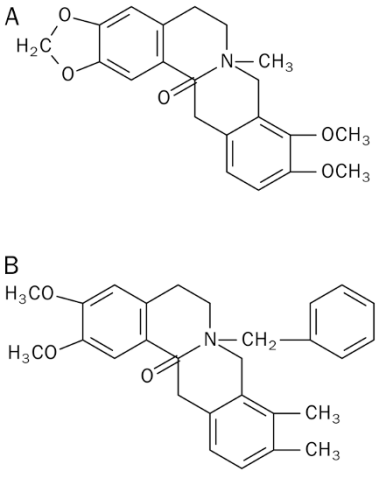

Figure 1. Chemical formula of ALL (A) and BTHP (B). ALL, an alkaloid, is extracted from *Corydalis decumbens* (Thunb) Pers. Papaveraceae and BTHP is a derivative of tetrahydropalmatine which is extracted from *Corydalis ambigua* (Pall) Cham et Schlecht.

electrophysiological action of ALL and BTHP on hERG channels expressed heterologously in human embryonic kidney (HEK) 293 cells using the whole-cell patch-clamp technique. Our findings provided detailed insight into the biophysical mechanism of hERG channel blockade by these two drugs.

Materials and methods

Transfection of HEK 293 cells

HEK 293 cells (American Type Culture Collection, Manassas, VA, USA) were maintained under 5% CO_2 in humidified air at 37 °C for biochemical analysis. Transient transfection of hERG channel cDNA plasmid pcDNA3.1 2.0 μg into the cultured cells was performed using Lipofectamine (Life Technologies, Gaithersburg, MD, USA) and the manufacturer's instructions. CD8 cDNA was co-transfected as a reporter gene (EBo-pCD vector, American Type Culture Collection). The CD8-positive cells were identified using Dynabeads (M-450 CD8, Invitrogen Co, CA, USA). The cells were harvested 48–72 h after transfection, and 25%–30% of transfection-positive cells were identified.

Reagents and solutions

Alpha-allocryptopine (ALL) was supplied by the Pharmaceutical Department of Lanzhou University (molecular weight 365, melting point 168 °C, a white crystal powder, 99.0% purity; its structure is shown in Figure 1A). It was dissolved in dimethyl sulfoxide (DMSO) to make a stock solution of 5.0 mmol/L. Benzyltetrahydropalmatine (BTHP) was supplied by China Pharmaceutical University (molecular weight 478.5, melting point 204 °C, white crystalline powder, over 99.0% purity; its structure is shown in Figure 1B). It was dissolved in distilled water to make a stock solution at 5 mmol/L. Dofetilide (Sequoia, Pangbourne, UK) was dissolved in DMSO to make stock solutions of 5 mmol/L, and the drug stock was added to a bath solution to produce the final concentrations mentioned in the Results section.

Patch clamp experiments

The HEK293 cells were bathed in a solution containing (in mmol/L) NaCl 140, KCl 4, $CaCl_2$ 2, $MgCl_2$ 1, HEPES 10, and glucose 5, and adjusted to a pH of 7.4 with NaOH. The current was recorded using the whole cell patch-clamp technique and a MultiClamp 700B amplifier (Axon Instruments). All of the signals were acquired at 5 kHz (Digidata 1322A, Axon Instruments). Patch pipettes were pulled from borosilicate glass on a P-97 horizontal puller (Sutter Instruments). The electrodes had a resistance of 1–3 MΩ.

To record K^+ currents, pipettes were filled with (in mmol/L) K-aspartame acid 140, MgATP 4, $MgCl_2$ 1, EGTA 10, GTP 0.1, and HEPES 10 and were adjusted to a pH of 7.3 with KOH. To ensure reproducibility, after the whole-cell conditions were established by rupturing the cell membrane, we allowed a dialysis period of 4 min before measuring any control records. During the dialysis period, we monitored the current-voltage relationships to ensure the stability and consistency of the recordings. The holding potential was -90 mV, and the interpulse interval was at least 15 s.

Data analysis and statistical methods

Off-line leak correction was performed on all of the amplitude data. Data are presented as the mean±SEM, with n representing the number of cells analyzed. pCLAMP version 9.2 (Axon Instruments) and Origin (Microcal Software) software were used for data analysis. Statistical significance was evaluated using a paired Student's t-test.

A $P<0.05$ was considered statistically significant. The concentration of drugs needed to yield a 50% blockade of the hERG current (IC_{50}) was obtained by fitting the data to a Hill equation: $I/I_0=1/[1+([C]/IC_{50})^{nH}]$, where I_0 and I are the current amplitudes measured in the absence and presence of drugs, respectively, [C] is the concentration of drugs in the external solution, and nH is the Hill coefficient.

Results

Concentration-dependent and time characteristics of I_{hERG} inhibition by ALL and BTHP

To define the concentration dependence of hERG channel current blockade by ALL and BTHP, we examined the effects of the two drugs on step and tail currents created from a holding potential of -90 mV. The membrane potential was stepped to +60 mV for 2000 ms and then repolarized to -40 mV for 3000 ms to elicit an outward tail current. The standard protocol was applied with a start-to-start interval of 15 s. The amplitude of the outward tail current in the reversal pulse partially exceeded the amplitude of the activating current due to slow activation, fast inactivation, and rapid recovery from inactivation[20, 21]. The current characteristics were stable by the fifth application of the protocol, which was considered the control for comparison with the currents recorded in the presence of the drugs. Figure 2A and 2B show representative

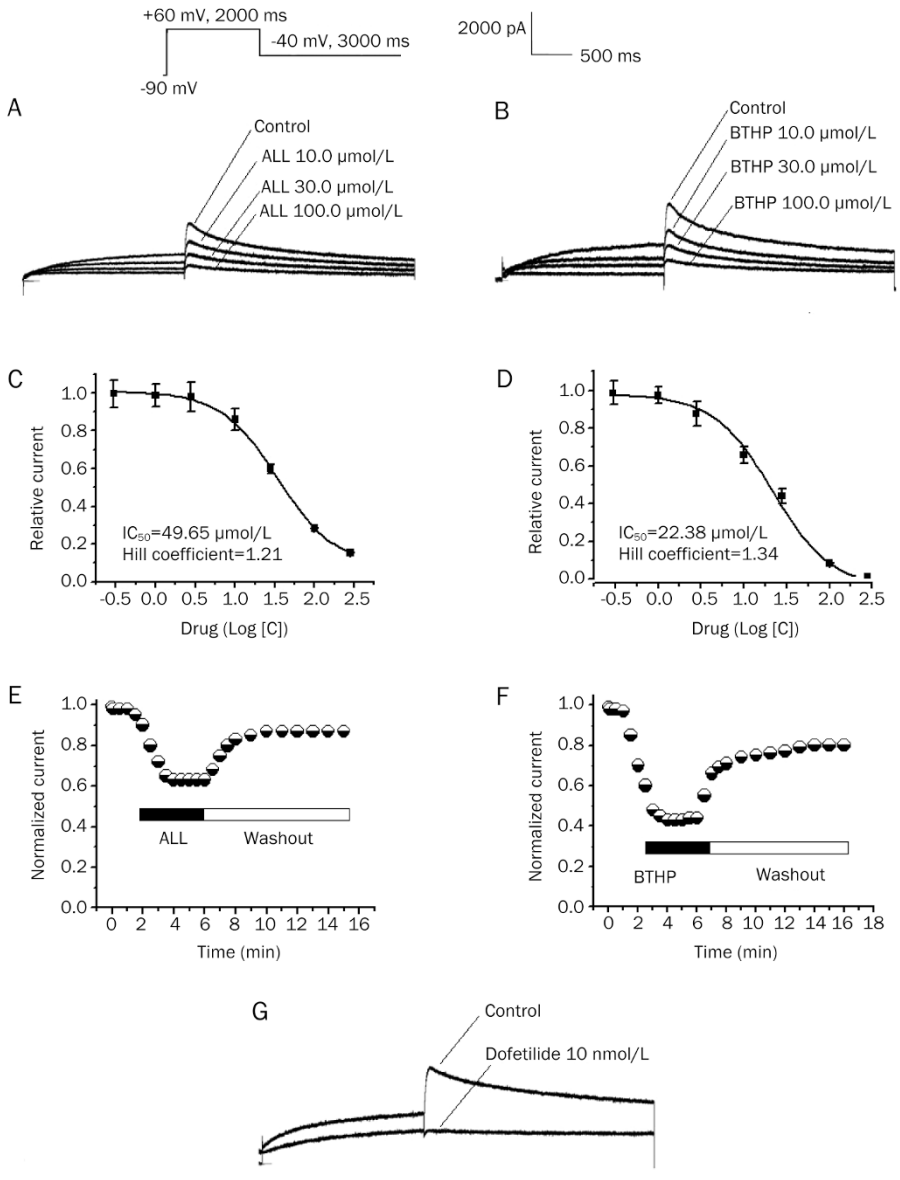

Figure 2. Inhibition of hERG channels by ALL and BTHP. (A and B) Representative current traces recorded from the same cell under control conditions and after superfusion with ALL and BTHP (10, 30, and 100 μmol/L). (C and D) Concentration-response relationship of the effects of ALL and BTHP on hERG peak tail currents (n=20). The IC_{50} of ALL was 49.65 μmol/L (95% CI: 34.75–64.54 μmol/L) with a Hill coefficient of 1.21 and the IC_{50} of BTHP was 22.38 μmol/L (95% CI: 13.56–31.20 μmol/L) with a Hill coefficient of 1.34. (E and F) Time course of hERG tail current inhibition by 30 μmol/L ALL and BTHP and washout effect (n=15). (G) The hERG current amplitude was decreased by dofetilide 10 nmol/L.

traces recorded from a single cell in which a range of concentrations of drugs was applied sequentially. During superfusion, the cell was continually stimulated to achieve saturation inhibition. Three different concentrations of ALL and BTHP, including 10, 30, and 100 μmol/L, were tested. Similar experiments were performed using seven different concentrations of the two drugs (*ie*, 0.3, 1.0, 3.0 10.0, 30.0, 100.0, and 300.0 μmol/L). The percent inhibition of the peak tail current was measured, and the mean data points were fitted with the Hill equation, as described in the Materials and Methods section. Figure 2C and 2D show plots of half-maximum inhibitory concentration (IC_{50}) values obtained for each drug; the IC_{50} value for BTHP was lower than that obtained for ALL. For ALL, IC_{50} was 49.65 μmol/L [95% confidence interval (CI): 34.75–64.54 μmol/L], and the Hill coefficient for the fit was 1.21; the IC_{50} of BTHP was 22.38 μmol/L (95% CI: 13.56–31.20 μmol/L), and the Hill coefficient was 1.34. Both drugs blocked the hERG current in a concentration-dependent manner. At a test potential of +60 mV, the hERG current amplitude was decreased by 10 nmol/L dofetilide (Figure 2G). Meanwhile, the current did not change in a DMSO control bath solution (<10%). Subsequent experiments were performed to identify time-dependent features of the development of I_{hERG} inhibition and washout action of the two drugs. After a control period of 2 min, which

demonstrated the stability of the experimental conditions, 30 μmol/L ALL was applied to perfuse the bath. The maximal inhibition with 38% of the control current occurred within 4 min (n=15), and a steady-state block was obtained with a small further increase in inhibition (less than 5%, Figure 2E). With the drug-free solution washout, the amplitude of I_{hERG} recovered to 90.0% of the control level in approximately 10 min. In another experiment, after a control period of 2 min, 30 μmol/L BTHP was applied instead of ALL. The maximal inhibition with 55% of the control current occurred within 4 min (n=15), and a steady-state block was obtained. The drug was washed out, and the inhibitory effect of BTHP was reversed with 78.5% recovery within 10 min (Figure 2F). When the cells were repetitively stimulated at a frequency of 0.1 Hz, the development of the hERG current blockade by ALL and BTHP occurred very rapidly; on washout, the effects recovered rapidly. This indicated an reversible blockade.

Voltage dependence of I_{hERG} inhibition by ALL and BTHP

Drugs that block ion channels often alter the voltage dependence or kinetics of channel gating. Therefore, we examined the effects of the drugs on the voltage dependence of activation and rectification and their effects on the kinetics of inactivation and deactivation. The voltage dependence of the drug-induced blockade of I_{hERG} was investigated by applying voltage commands of 5000 ms duration from a holding potential of -90 mV to a range of test potentials, followed by a repolarizing step to -40 mV for 3000 ms to elicit tail currents. The measurements of step and tail currents were made in the control group and in the presence of 30 μmol/L ALL or 30 μmol/L BTHP. Both the step and tail current amplitudes were dramatically reduced by the two drugs (Figure 3A). At a test potential of +60 mV, the step current was reduced from 51.2±3.2 pA/pF to 34.6±2.9 pA/pF by ALL and to 24.5±2.4 pA/pF by BTHP. The tail current was reduced from 143.5±7.8 pA/pF to 97.1±5.6 pA/pF by ALL and to 65.3±4.2 pA/pF by BTHP (P<0.01, n=15, Figure 3B). The peak amplitudes of the tail currents were reduced by 32.3%±1.6% (ALL) and 54.5%±2.3% (BTHP).

Figure 3C and 3D show a representative current-voltage relationship for I_{hERG} step and tail currents before and after using the drugs. The hERG currents were activated at potentials gearter than -40 mV. The amplitude of the outward step current increased with depolarization up to 0 mV and decreased with further depolarization, which is typical for an inward rectifying property of the hERG current. The I–V curve of the step current showed a bell-shaped relationship, and the tail current amplitude was steady-state after test pulses of +30 mV or above. The step current densities were

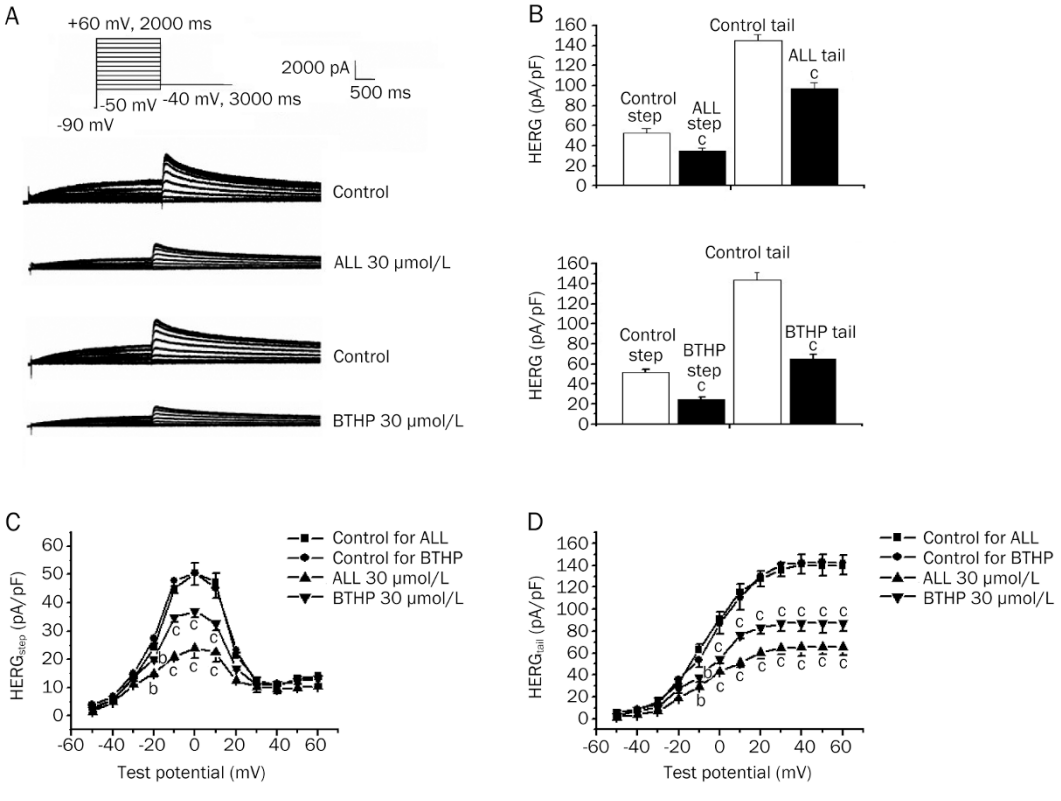

Figure 3. Inhibition effect of ALL and BTHP on step and tail currents by repolarizing pulse of -40 mV. (A) Representative current traces recorded under control conditions and after superfusion with ALL and BTHP (30 μmol/L). (B) The inhibitory effect of drugs (30 μmol/L) on repolarizing pulse of -40 mV is shown and the peak amplitude of step current was reduced. At test potential of +60 mV, the step current was reduced from 51.2±3.2 pA/pF to 34.6±2.9 pA/pF by ALL and to 24.5±2.4 pA/pF by BTHP and the magnitude of I_{hERG} tail was from 143.5±7.8 to 97.1±5.6 pA/pF by ALL and to 65.3±4.2 pA/pF by BTHP. (C and D) Summary of ALL and BTHP on current density-voltage relationship of step and tail currents. ^bP<0.05, ^cP<0.01, n=15.

decreased by the two drugs between -20 mV and +20 mV. At a potential of -10 mV, the tail current densities were significantly decreased by both drugs (P<0.05 or P<0.01), while the blocking effects of the drugs on the tail current resulted in a slight change at more positive potentials. A reason for this might be the low amplitude of the current at these potentials.

Figure 4 shows the inhibition effects of ALL and BTHP on the tail currents using a repolarizing pulse of -110 mV. The current traces were recorded under control conditions and after superfusion with ALL 30 μmol/L and BTHP 30 μmol/L. At a test potential of +60 mV, the tail current was reduced from -190.3±11.7 pA/pF to -137.4±9.9 pA/pF by ALL and to -105.4±7.8 pA/pF by BTHP (P<0.01, n=15). The peak amplitude of the tail current was reduced by 27.8%±3.1% (ALL) and 45.6%±2.8% (BTHP) (Figure 4A–4C). A significant reduction in the tail current was first observed at -10 mV, and the inhibition gradually became more significant with increasingly positive potentials, which was different from the inhibition feature of the tail current elicited at a repolarization potential of -40 mV. Neither drug showed the maximal blockade of the tail current at a repolarization potential of -110 mV within the range of test potentials from -10 mV to +60 mV.

The effects of ALL and BTHP on the rectification characteristics of hERG currents are shown in Figure 5A and 5B. The I–V relationship for the steady-state exposure of the two drugs exhibited a similar pattern to the inward rectification characteristics of the control between -70 mV to +20 mV. Conversely, the rectification curve by 30 μmol/L BTHP diverged slightly lower over +10 mV of test potentials (Figure 5C and 5D). The rectification characteristics of hERG may be increased by BTHP in the range of these potentials.

The effects of ALL and BTHP on the activation and deactivation of the I_{hERG} channel

To understand the apparent effect of the drugs in greater detail, the steady-state activation of I_{hERG} was studied and fitted with the Boltzmann equation: $G/G_{max}=1/(1+\exp[(V_m-V_{1/2})/k])$[22]. The voltage dependence of the current activation was assessed using standard tail current analysis. The cells were depolarized to potentials in the range of -50 mV to +60 mV for 2000 ms and the tail current was recorded at -40 mV for 2000 ms. The voltage-dependent activation curves for I_{hERG} for the control and the drugs are plotted in Figure 6A and 6B. Neither ALL nor BTHP exerted significant effects on the half-activated voltage ($V_{1/2}$) and activated curve slope (k) when compared with the control. Neither drug significantly altered the slope factor for the fitted relationships. The small and similar effects of both drugs suggest that the effects on the voltage dependence of I_{hERG} activation cannot account for the greater variation when using ALL compared to BTHP. The I_{hERG} tails were fitted with a single-exponential equation (I=Aexp($-t/\tau$)+C). The mean values of the activation time constants in the control and the presence of 30 μmol/L ALL or 30 μmol/L BTHP were not significantly different (Figure 6C and 6D). It is suggested that neither drug has a statistically significant effect on the voltage dependence of hERG activation time constants

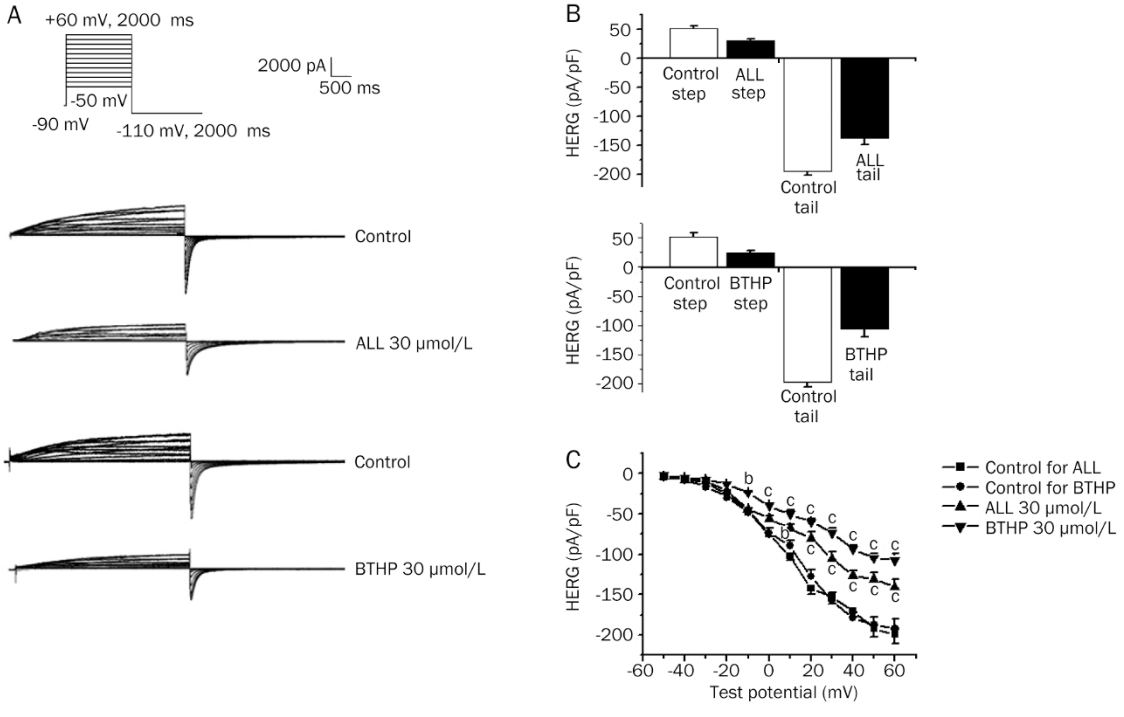

Figure 4. Inhibitory effect of ALL and BTHP on step and tail currents by reploarizing pulse of -110 mV. (A) Representative current traces recorded under control conditions and after superfusion with ALL and BTHP (30 μmol/L). (B) The inhibitory effect of drugs (30 μmol/L) on reploarizing pulse of -110 mV is shown and the magnitude of I_{hERG} tail was reduced from -190.3±11.7 to -137.4±9.9 pA/pF by ALL and to -105.4±7.8 pA/pF by BTHP. (C) Summary of ALL and BTHP on current density-voltage relationship of tail currents. ^bP<0.05, ^cP<0.01, n=15.

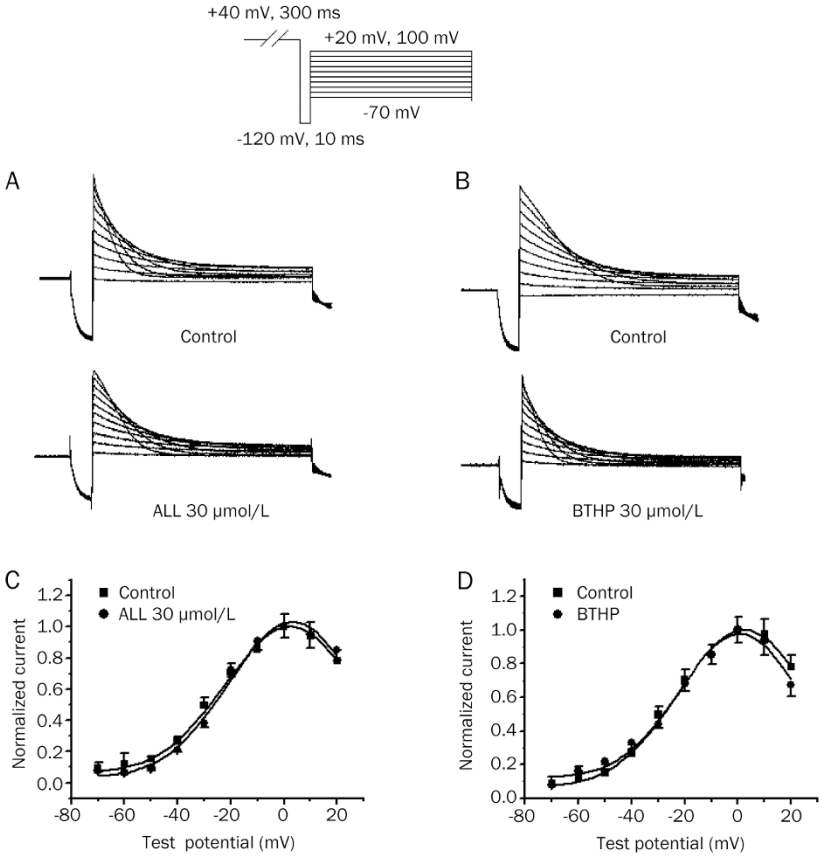

Figure 5. Effects of ALL and BTHP on rectification characteristics of hERG current. (A and B) Representative current traces before and after exposure to two drugs are shown. (C and D) *I–V* relationship for steady-state exposure to two drugs exhibits similar pattern to inward rectification characteristics of control between -70 mV to +20 mV, but rectification curve by 30 μmol/L BTHP diverges slightly lower than that of control.

under our experimental conditions.

The deactivation procedure of the I_{hERG} tails were fitted with a bi-exponential equation (I=A1exp(-t/τ1)+A2exp(-t/τ2)+C[23, 24]. The slow deactivation time course of the I_{hERG} tails was accelerated by BTHP, but not by ALL (Figure 6E). At a test potential of -40 mV, the mean values of the slow deactivation time constants (τ2) in the control and in the presence of 30 μmol/L BTHP were 1450.2±43.6 ms and 1060.3±47.5 ms, respectively (P<0.01, n=15). The mean values of the fast deactivation time constants (τ1) before and after 30 μmol/L BTHP were 315.3±21.7 ms and 298.8±14.3 ms, respectively (Figure 6F). The results suggested that BTHP mainly accelerated the slow deactivation procedure of the hERG channel. The shortened deactivation in the presence of BTHP suggested that the closure of the activation gate was delayed when the drug was bound to the channel. The results showed that neither the fast nor slow deactivation time course of the I_{hERG} tails was significantly altered by 30 μmol/L ALL (Figure 6E). To determine whether the deactivated kinetics were changed, the fast and slow time constant proportions [A1/(A1+A2) and A2/(A1+A2)] under each test potential were calculated. The results showed that the fast and slow time constant proportions under each test potential did not change before or after exposure to the two drugs (Figure 6G and 6H).

The effects of ALL and BTHP on I_{hERG} availability and inactivation time-course

Two different protocols were used to analyze the effects of ALL and BTHP on the steady-state and fast inactivation of the hERG current. First, the voltage dependence of the steady-state inactivation/availability was measured using a condition pulse depolarization to +20 mV for 1000 ms and short pulses to potentials ranging from -120 mV to +20 mV for 20 ms with 10 mV-increments to recover the channels from inactivation, followed by a test potential of +20 mV for 1500 ms. In the protocol, we set the second voltage step pulse duration to 20 ms, which was well beyond 4 times the time constants of the recovery from inactivation for hERG channels; this ensured almost full recovery from inactivation by the end of the pulse. The current amplitudes were normalized and fitted to a Boltzmann function, I/I_{max}=1/(1+exp[-($V_{1/2}$–V_m)/k]), where I/I_{max} is the relative current, $V_{1/2}$ is the half-maximum inactivation voltage, V_m is the test membrane potential, and k is the slope factor. The experiment was performed in the absence and presence of the drug. Compared to the control, $V_{1/2}$ of the steady-state inactivation curve of the hERG current shifted to a more negative potential (from -54.13±2.42 mV to -78.89±2.38 mV) with 30 μmol/L BTHP (P<0.01, n=17), while it showed

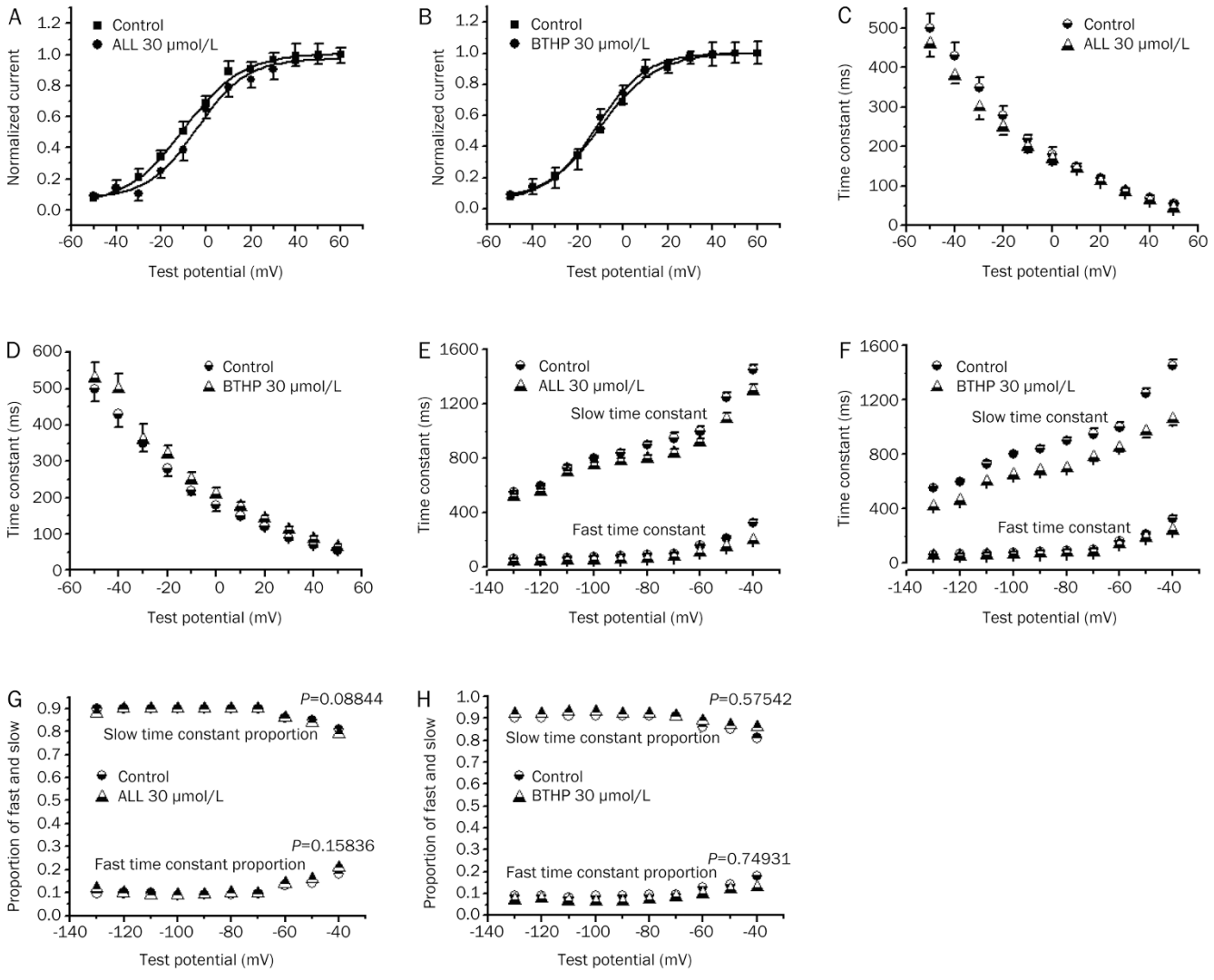

Figure 6. Effects of ALL and BTHP on the activation and deactivation of hERG current. Normalized tail currents were displayed as a function of the preceding test pulse voltages and fitted with a Boltzmann function. Steady-state activation curves are shown differently in the absence of and presence of 30 μmol/L ALL and 30 μmol/L BTHP (n=17, A and B). Time constants of activation were not markedly different before and after exposure to two drugs (C and D). Fast time constants of deactivation were similar before and after exposure to two drugs. The slow time constants of deactivation were shortened by 30 μmol/L BTHP, but not affected by 30 μmol/L ALL (E and F). The fast and slow time constant proportion under each test potential is not changed before and after exposure to two drugs, respectively (G and H).

only a slight change with 30 μmol/L ALL (from -55.33±3.14 mV to -57.38±2.52 mV) (Figure 7A–7D).

In the second approach, the voltage dependence of the time course of fast inactivation was investigated. From a holding potential of -90 mV, a condition test pulse of +50 mV for 1500 ms was applied to inactivate the channel; short pulses to -100 mV for 10 ms and voltage steps to potentials ranging from -20 mV to +60 mV for 1500 ms in 10-mV increments were then used to elicit large outward inactivating currents. The inactivating currents were fitted with single exponential functions to obtain a time constant[25, 26]. Compared to the control, the time constants of fast inactivation were significantly shortened by 30 μmol/L BTHP at a range of the various potentials, except at +60 mV (P<0.01, n=17). Similarly, the time constant of fast inactivation was shortened by 30 μmol/L ALL at -20 and 0 mV, but there was a slight change at +10 mV (Figure 7E–7H). Considered collectively, these results suggested that the two drugs had similar effects on the availability or inactivation time-course. Furthermore, BTHP caused a more negative potential shift of $V_{1/2}$ and a shorter time constant than ALL.

The effects of ALL and BTHP on I_{hERG} recovery of channel inactivation

Recovery from inactivation was observed as a time-dependent initial increase in current amplitude at potentials from -120 mV to -50 mV for 3000 ms after a conditioning pulse of +50 mV for 1500 ms. The effects of ALL and BTHP on I_{hERG} recovery of channel inactivation are shown in Figure 8A and 8B. The tail

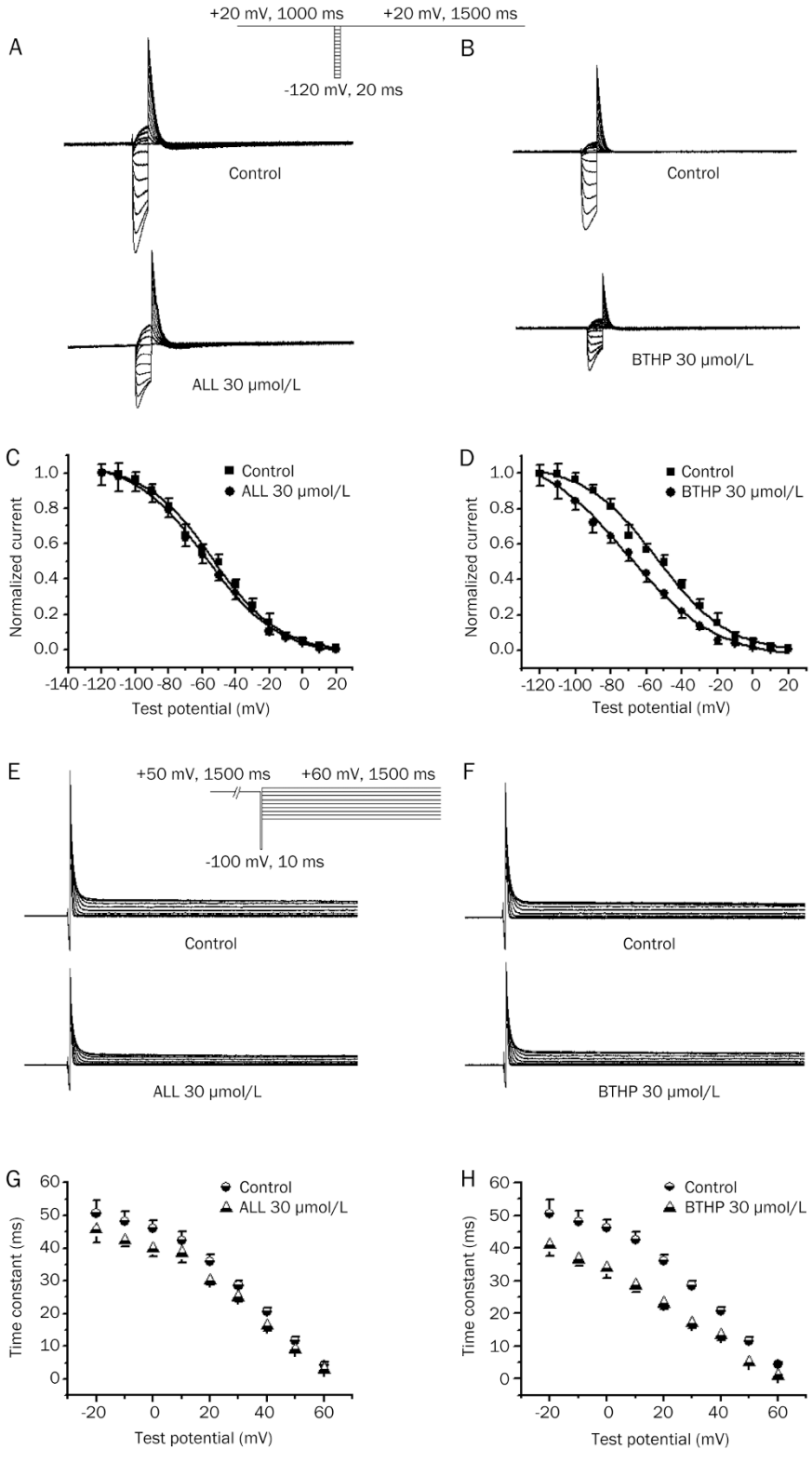

Figure 7. Effects of ALL and BTHP on steady-state inactivation and fast inactivation of hERG current. $V_{1/2}$ of the steady-state inactivation curve of hERG current showed more negative shift by 30 μmol/L BTHP (from -54.13±2.42 mV to -78.89±2.38 mV) (P<0.01, n=17) , while showed only slight change by 30 μmol/L ALL (from -55.33±3.14 mV to -57.38±2.52 mV) (A–D). Inactivating currents were fitted with single exponential functions to obtain time constants. Voltage dependence of time course of fast inactivation was investigated. Compared with control, time constant of fast inactivation was significantly shortened by 30 μmol/L BTHP (P<0.01, n=17) but was only slightly shortened by 30 μmol/L ALL over +10 mV (E–H).

currents were fitted by a single exponential function[23]. Compared with the control, the time constants for recovery from inactivation were significantly lengthened over -80 mV potentials after exposure to ALL. For BTHP, the time constants for recovery from inactivation were significantly lengthened over -90 mV potentials. Meanwhile, a more pronounced prolongation of the time constant was observed with BTHP (4.35 times the control) than with ALL (2.45 times the control) at a test potential of -50 mV (Figure 8C and 8D).

The effects of ALL and BTHP on the I_{hERG} current with an action potential waveform pulse

The characteristics of hERG currents during an action potential (AP) were tested using the AP-clamp technique[27, 28]. An AP waveform of a human ventricular cell was stimulated at a 400 ms cycle length, digitized at 10 kHz and stored. The AP waveform was used as a command signal under voltage-clamp conditions. At least 10 consecutive waveforms were applied to reach stable electrical activity. The peak current densities, as a function of the voltage applied, showed a decrease of 43.22%±5.3% with ALL and 56.78%±2.7% with BTHP during the late phase of the action potential (n= 6, P<0.01). The densities were not significantly different between the control and the two drugs during the early phase of the action potential (Figure 9).

Discussion

The inhibition effects of ALL and BTHP on I_{hERG} and clinical implications

It is very important to search for new antiarrhythmic agents because many antiarrhythmic drugs increase the tendency for heart arrhythmias and the occurrence of TdP ventricular tachycardias. It is of particular interest to investigate the effects of antiarrhythmic drugs on the hERG potassium channel. Likewise, a blockade of hERG channels by various drugs has been investigated previously (such drugs include azimilide, amiodarone, terikalant, dofetilide, clofilium and its analogue LY97241, haloperidol, terfenadine and carvedilol)[29–35].

The major finding of this study is that two commonly prescribed Chinese herb drugs, *ie*, ALL and BTHP, potently block the hERG current in a voltage- and concentration-dependent manner. This is, to our knowledge, the first study showing that ALL and BTHP are potent hERG blockers. Previous studies have indicated that BTHP has antiarrhythmic effects in various animal models[17–19]. The electrophysiological effect of BTHP is related to the prolongation of the action potential duration, similar to that of class III antiarrhythmic agents. In previous studies, we found that BTHP could inhibit both

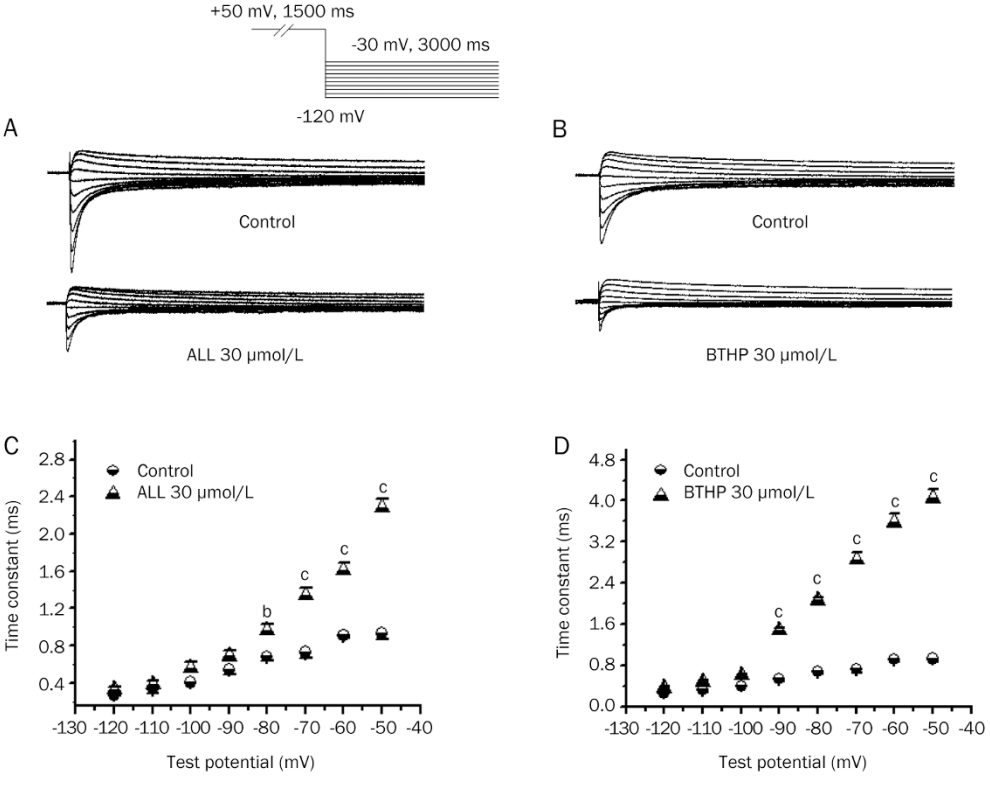

Figure 8. Effects of ALL and BTHP on voltage dependence of recovery of inactivation of hERG currents. Recovery from inactivation traces was observed as the time-dependent initial increase in current amplitude at potentials from -120 mV to -50 mV for 3000 ms after condition pulse at +50 mV for 1500 ms (A and B). Tail currents were fitted by a single-exponential function. For two drugs, the time constants for recovery from inactivation were significantly lengthened over -80 mV test potentials compared to control with more significant acceleration of prolongation by 30 μmol/L BTHP (C and D). ^{b}P<0.05, ^{c}P<0.01 *vs* control, n=17.

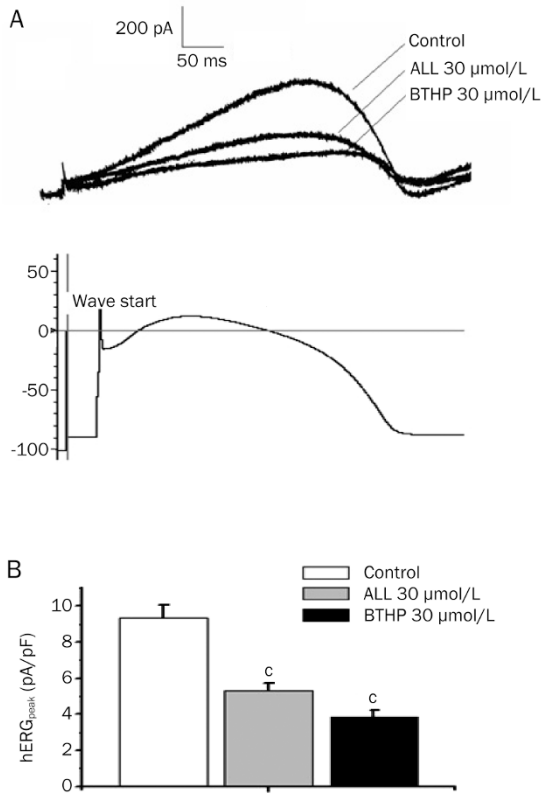

Figure 9. Effects of ALL and BTHP on characteristics of hERG current with action potential waveform pulse. Digitized action potential waveform was used as command potential. (A) Representative current tracings before and after exposure to two drugs. (B) The current densities by two drugs, as a function of the voltage applied, showed marked decrease compared to control during late phase of action potential, especially for peak current. The peak current densities, as a function of the voltage applied, showed a decrease of 43.22%±5.3% of ALL and 56.78%±2.7% of BTHP during the late phase of action potential (n=6, B), while they were not significantly different during early phase of action potential. ^cP<0.01 *vs* control.

I_{Kr} and the "slow" delayed rectifier potassium current (I_{Ks}) without any obvious selectivity[36–39]. In other reports, we demonstrated that the threshold doses of aconitine and calcium chloride that induced ventricular ectopic beats, ventricular tachycardia and ventricular fibrillation in rats were increased by ALL. The electrophysiological measurements of ALL showed a prolongation of APD in the rabbit heart[14, 15]. We have also found that ALL exerted an inhibition effect on the transient outward potassium current (I_{to}) in a frequency-dependent manner and decreased the transmural gradient of I_{to}[16]. Both ALL and BTHP have a basic isoquinoline constitution (Figure 1) and belong to isoquinoline alkaloid categorization. Other reports showed that several isoquinoline alkaloid agents also had antiarrhythmic effects as a series of quaternary ammonium type of antiarrhythmic drugs[40–47]. Therefore, we can speculate that ALL and BTHP, as potential antiarrhythmic agents, may be brought into use in the near future.

The effects of ALL and BTHP on the I_{hERG} channel gating mechanism

As repolarization proceeds, a transient increase in the hERG current occurs due to the fast recovery from inactivation and slow deactivation, which electively repolarizes the cardiac cell[48, 49]. At negative repolarizing voltages, prominent tail currents are produced after the channels reopen and rapidly recover from inactivation, before closing at a slow rate[50–52]. Rapidly inactivation characteristics of channel makes hERG operate as an inward rectifier, although it has 6 membrane-spanning domains and regions typical of depolarization-activated channels[21]. It is necessary to investigate the effect of a new drug on hERG kinetic characteristics. In our experiment, a blockade of the hERG channel by both drugs led to several features in the inactivation state, deactivation states and during recovery of fast inactivation. The activation state and inward rectifier channel were not markedly affected. The $V_{1/2}$ of the steady-state inactivation curve of the hERG current showed a significantly negative shift with BTHP (BTHP: -78.89±2.38 mV *vs* Ctrl: -54.13±2.42 mV, P<0.001) but not ALL (ALL: -57.38±2.52 mV *vs* Ctrl: -55.33±3.14 mV). The time constants of fast inactivation were significantly shortened with BTHP, while the time constants were slightly changed by 30 μmol/L ALL from -20 mV–0 mV. Meanwhile, the slow time constants of deactivation were shortened with BTHP, but not with ALL. Furthermore, the time constants for recovery from inactivation were significantly lengthened by both drugs at all potentials compared to the control. This may be the major reason for the blockade effect of ALL on the hERG current, despite the more significant acceleration with BTHP. Collectively, these reasons may explain the stronger inhibition of BTHP on the hERG current, while the hERG currents were blocked by both drugs. BTHP blocked the tail currents (-40 mV) by 45.5%±2.3%, and ALL blocked the tail currents by 33.3%±1.6%. BTHP blocked the tail currents (-110 mV) by 45.6%±2.8%, and ALL blocked the tail currents by 27.8%±3.1%.

The effects of ALL and BTHP on the I_{hERG} current with the action potential clamp

The action potential clamp technique offers a valuable approach to the study of the dynamics of specific currents because the currents actually occur during the action potential. This tool is also used to study the dynamic properties of membrane ionic currents[28, 53, 54]. Similar to results of the voltage-clamp, the current densities showed a marked decrease of 49.2% with ALL blockade and 61.5% with BTHP blockade during the late phase of the action potential. The densities were not significantly different between the control group and the two drugs during the early phase of the action potential. Therefore, we presume that the drugs only reduced the current densities of hERG rather than the dynamic properties of the hERG current during the action potential.

Limitations of the present study

As we know, the I_{Kr} current is generated by the hERG K_v

α-subunit, which is modulated *in vitro* by single transmembrane domain ancillary subunits MiRP1 (encoded by KCNE2, respectively). KCNE2 has been linked to hereditary arrhythmias and pro-arrhythmic drug sensitivity[55, 56]. In this article, we have focused on the functional electrophysiological effects of ALL and BTHP on the HERG current. It is necessary to investigate the effects of the two drugs on co-expression experiments with HERG and KCNE2.

Acknowledgements

This study was supported by grants from the National Natural Science Foundation of China (No 81170177, No 30770901).

The authors would like to thank Prof Silvia G PRIORI from Molecular Cardiology, Fondazione Salvatore Maugeri IRCCS, at the University of Pavia in Italy for generously providing the hERG plasmid.

Author contribution

Yang LI designed the research; Kun LIN, Yu-qi LIU, Jin-liao GAO, and Bin XU performed research; Yi-cheng FU and Yu CHEN contributed new reagents or analytic tools; Qiao XUE and Yang LI analyzed data; Yang LI and Yu-qi LIU wrote the paper.

References

1 Sanguinetti MC, Jiang C, Curran ME, Keating MT. A mechanistic link between an inherited and an acquired cardiac arrhythmia: hERG encodes the IKr potassium channel. Cell 1995; 81: 299–307.
2 Trudeau MC, Warmke JW, Ganetzky B, Robertson GA. hERG, a human inward rectifier in the voltage-gated potassium channel family. Science 1995; 269: 92–5.
3 Royer A, Demolombe S, El Harchi A, Le Quang K, Piron J, Toumaniantz G, *et al*. Expression of human ERGK$^+$ channels in the mouse heart exerts anti-arrhythmic activity. Cardiovasc Res 2005; 65: 128–37.
4 Spector PS, Curran ME, Keating MT, Sanguinetti MC. Class III antiarrhythmic drugs block HERG, a human cardiac delayed rectifier K$^+$ channel. Open-channel block by methanesulfonanilides. Circ Res 1996; 78: 499–503.
5 Kiehn J, Thomas D, Karle CA, Schöls W, Kübler W. Inhibitory effects of the class III antiarrhythmic drug amiodarone on cloned HERG potassium channels. Naunyn-Schmiedeberg's Arch Pharmacol 1999; 359: 212–9.
6 Alvarez PA, Pahissa J. QT alterations in psychopharmacology: proven candidates and suspects. Current Drug Safety 2010; 5: 97–104.
7 Mitcheson JS, Chen J, Lin M, Culberson C, Sanguinetti MC. A structural basis for drug-induced long QT syndrome. Proc Natl Acad Sci U S A 2000; 97: 12329–33.
8 Scherer CR, Lerche C, Decher N, Dennis AT, Maier P, Ficker E, *et al*. The antihistamine fexofenadine does not affect I_{Kr} currents in a case report of drug-induced cardiac arrhythmia. Br J Pharmacol 2002; 137: 892–900.
9 Lehtonen A, Fodstad H, Laitinen-Forsblom P, Toivonen L, Kontula K, Swan H. Further evidence of inherited long QT syndrome gene mutations in antiarrhythmic drug-associated torsades de pointes. Heart Rhythm 2007; 4: 603–7.
10 Ye F, Feng F, Liu W. Alkaloids from *Macleaya cordata*. Zhongguo Zhong Yao Za Zhi 2009; 34: 1683–6.
11 Chen YZ, Liu GZ , Shen Y, Chen B, Zeng JG. Analysis of alkaloids in *Macleaya cordata* (Willd) R Br. Using high-performance liquid chromatography with diode array detection and electrospray ionization mass spectrometry. J Cromatogr A 2009; 1216: 2104–10.
12 Liu H, Wang J, Zhao J, Lu S, Wang J, Jiang W, *et al*. Isoquinoline alkaloids from *Macleaya cordata* active against plant microbial pathogens. Nat Prod Commun 2009; 4: 1557–60.
13 Du F, Wang S, Xie Z. Concentration of four alkaloids in the aerial parts of *Eomecon chionantha* from different month in year. Zhong Yao Cai 2000; 23: 189–90.
14 Li Y, Wang S, Liu Y, Li Z, Yang X, Wang H, *et al*. Effect of alpha–allocryptopine on transient outward potassium current in rabbit ventricular myocytes. Cardiology 2008; 111: 229–36.
15 Liu M, Li Y, Wen Y. The effect of allocryptopine on arrhythmia and monophasic action potential in animal models. Chin J Mult Organ Dis Elder 2006; 5: 48–50.
16 Li Y, Wang L, Cheng R. Effects of allocryptopine on arrhythmia of animals and action potential of the papillary muscles of guinea pigs. Chin J Mult Organ Dis Elder 2005; 4: 123–6.
17 Zhang JS, Yao WX, Xia GJ, Jiang MX, Huang YC. Antiarrhythmic effect of benzyltetrahydropalmatine on several animal model. J Huazhong Univ Sci Tech (Med Sci) 2004; 24: 433–6.
18 Li Y, Fu LY, Yao WX, Xia GJ, Jiang MX. Effects of benzyltetrahydropalmatine on two components of the delayed rectifier K$^+$ current in Guinea pig ventricular myocytes. Cardiovasc Drugs Ther 2002; 16: 317–25.
19 Xia GJ, Yao WX, Liu XK, Jiang MX. Effects of benzyltetrahydropalmatine on ischemia reperfusion with monophasic action potential. Yao Xue Xue Bao 1990; 25: 293–6.
20 Kiehn J, Lacerda AE, Brown AM. Pathways of HERG inactivation. Am J Physiol 1999; 277: H199–210.
21 Spector PS, Curran ME, Zou A, Keating MT, Sanguinetti MC. Fast inactivation causes rectification of the I_{Kr} channel. J Gen Physiol 1996; 107: 611–9.
22 Nakajima T, Furukawa T, Hirano Y, Tanaka T, Sakurada H, Takahashi T, *et al*. Voltage-shift of the current activationin HERG S4 mutation (R534C) in LQT2. Cardiovasc Res 1999; 44: 283–93.
23 Bett GC, Zhou Q, Rasmusson RL. Models of HERG gating. Biophysical J 2011; 101: 631–42.
24 Choi SH, Shin TJ, Hwang SH, Lee BH, Kang J, Kim HJ, *et al*. Ginsenoside Rg(3) decelerates hERG K$^+$ channel deactivation through Ser631 residue interaction. Eur J Pharmacol 2011; 663: 59–67.
25 Milnes JT, Witchel HJ, Leaney JL, Leishman DJ, Hancox JC. Investigating dynamic protocol-dependence of hERG potassium channel inhibition at 37 degrees C: Cisapride versus dofetilide. J Pharmacol Toxicol Methods 2009; 61: 178–91.
26 Nakajima T, Furukawa T, Tanaka T, Katayama Y, Nagai R, Nakamura Y, *et al*. Novel mechanism of HERG current suppression in LQT2: shift in voltage dependence of HERG inactivation. Circ Res 1998; 83: 415–22.
27 McPate MJ, Zhang H, Adeniran I, Cordeiro JM, Witchel HJ, Hancox JC. Comparative effects of the short QT N588K mutation at 37 degrees C on hERG K$^+$ channel current during ventricular, Purkinje fibre and atrial action potentials: an action potential clamp study. J Physiol Pharmacol 2009; 60: 23–41.
28 Zhang YH, Colenso CK, Sessions RB, Dempsey CE, Hancox JC. The hERG K$^+$ channel S4 domain L532P mutation: Characterization at 37 °C. Biochim Biophys Acta 2011; 1808: 2477–87.
29 Busch AE, Eigenberger B, Jurkiewicz NK, Salata JJ, Pica A, Suessbrich H, *et al*. Blockade of HERG channels by the class III antiarrhythmic azimilide: mode of action. Br J Pharmacol 1998; 123: 23–30.
30 Jurkiewicz NK, Wang J, Fermini B, Sanguinetti MC, Salata JJ. Mechanism of action potential prolongation by RP 58866 and its

active enantiomer, terikalant. Block of the rapidly activating delayed rectifier K^+ current, I_{Kr}. Circulation 1996; 94: 2938–46.
31 Kiehn J, Lacerda AE, Wible B, Brown AM. Molecular physiology and pharmacology of HERG. Single-channel currents and block by dofetilide. Circulation 1996; 94: 2572–9.
32 Suessbrich H, Schönherr R, Heinemann SH, Lang F, Busch AE. Specific block of cloned hERG channels by clofilium and its tertiary analog LY97241. FEBS Lett 1997; 414: 435–8.
33 Suessbrich H, Schönherr R, Heinemann SH, Attali B, Lang F, Busch AE. The inhibitory effect of the antipsychotic drug haloperidolon HERG potassium channels expressed in *Xenopus* oocytes. Br J Pharmacol 1997; 120: 968–74.
34 Suessbrich H, Waldegger S, Lang F, Busch AE. Blockade of HERG channels expressed in *Xenopus* oocytes by the histamine receptor antagonists terfenadine and astemizole. FEBS Lett 1996; 385: 77–80.
35 Karle CA, Kreye VA, Thomas D, Röckl K, Kathöfer S, Zhang W, *et al*. Antiarrhythmic drug carvedilol inhibits HERG potassium channels. Cardiovasc Res 2001; 49: 361–70.
36 Yao WX, Xia GJ, Zeng WZ, Jiang MX. Effects of benzyltetrahydropalmatine on delayed after depolarization and triggered activity and rabbit His-bundle electrogram. Zhongguo Yao Li Xue Bao 1990; 11: 141–3.
37 Zeng WZ, Xia GJ, Yao WX, Zong XG, Jiang MX. Effects of benzyltetrahydropalmatine on action potentials of myocardium and transmembrane K^+ and Ca^{2+} currents in Purkinje fibers. Zhongguo Yao Li Xue Bao 1990; 11: 314–7.
38 Tong QS, Xia GJ, Yao WX, Jiang MX, Bai XC, Bao YD. Blocking effects of benzyltetrahydropalmatine on delayed rectified K^+ currents expressed in *Xenopus* oocytes and in toad oocytes. Yao Xue Xue Bao 1996; 31: 867–71.
39 Li Y, Fu LY, Yao WX, Xia GJ, Jiang MX. Effects of benzyltetrahydropalmatine on potassium currents in guinea pig and rat ventricular myocytes. Acta Pharmacol Sin 2002; 23: 612–6.
40 Xia JS, Li Z, Dong JW, Tu H, Zeng FD. Dauricine-induced changes in monophasic action potentials and effective refractory period of rabbit left ventricle *in situ*. Acta pharmacol Sin 2002; 23: 371–5.
41 Qian JQ. Cardiovascular pharmacological effects of bisbenzylisoquinolineal kaloid derivatives. Acta Pharmacol Sin 2002; 23: 1086–92.
42 Morales MA, González E, Torres R, Martínez JL. Cardiodepressor effects of 7-O-demethylisothalicberine, bisbenzylisoquinolinealkaloid isolated from *Berberis chilensis*. Arch Med Res 1993; 24: 177–81.
43 Wang JL, Nong Y, Jing MX. Effects of liensinine on haemodynamics in rats and the physiologic properties of isolated rabbit atria. Yao Xue Xue Bao 1992; 27: 881–5.
44 Wang LH, Yu CH, Fu Y, Li Q, Sun YQ. Berberine elicits anti-arrhythmic effects via IK1/Kir2.1 in the rat type 2 diabetic myocardial infarction model. Phytother Res 2011; 25: 33–7.
45 Li BX, Yang BF, Zhou J, Xu CQ, Li YR. Inhibitory effects of berberine on I_{K1}, I_K, and hERG channels of cardiac myocytes. Acta Pharmacol Sin 2001; 22: 125–31.
46 Wang XX, Chen JZ, Cheng LX, Zhou LL. Effect of tetradrine on electrophysilogic changes caused by rising of left ventricular preload in guinea pigs. Zhongguo Zhong Yao Za Zhi 2003; 28: 1054–6.
47 Xu CQ, Dong DL, Du ZM, Chen QW, Gong DM, Yang BF. Comparison of the anti-arrhythmic effects of matrine and berbamine with amiodarone and RP58866. Yao Xue Xue Bao 2004; 39: 691–4.
48 Zhou Q, Zygmunt AC, Cordeiro JM, Siso-Nadal F, Miller RE, Buzzard GT, *et al*. Identification of Ikr kinetics and drug binding in native myocytes. Ann Biomed Eng 2009; 37: 1294–309.
49 Wang J, Myers CD, Robertson GA. Dynamic control of deactivation gatingby a soluble amino-terminal domain in HERG K^+ channels. J Gen Physiol 2000; 115: 749–58.
50 Trudeau MC, Warmke JW, Ganetzky B, Robertson GA. HERG, a human inward rectifier in the voltage-gated potassium channel family. Science 1995; 269: 92–5.
51 Gustina AS, Trudeau MC. hERG potassium channel gating is mediated by N- and C-terminal region interactions. J Gen Physiol 2011; 137: 315–25.
52 Smith PL, Baukrowitz T, Yellen G. The inward rectification mechanism of the HERG cardiac potassium channel. Nature 1996; 379: 833–6.
53 Fougere RR, Es-Salah-Lamoureux Z, Rezazadeh S, Eldstrom J, Fedida D. Functional characterization of the LQT2-causing mutation R582C and the associated voltage-dependent fluorescence signal. Heart Rhythm 2011; 8: 1273–80.
54 Du CY, Adeniran I, Cheng H, Zhang YH, El Harchi A, McPate MJ, *et al*. Acidosis impairs the protective role of hERG K^+ channels against premature stimulation. J Cardiovasc Electrophysiol 2010; 21: 1160–9.
55 Park KH, Kwok SM, Sharon C, Berga R, Sesti F. N-Glycosylation-dependent block is a novel mechanism for drug-induced cardiac arrhythmia. FASEB J 2003; 17: 2308–9.
56 Abbott GW, Goldstein SA. Potassium channel subunits encoded by the KCNE gene family: physiology and pathophysiology of the MinK-related peptides (MiRPs). Mol Interv 2001; 1: 95–107.